Different Conformers and Protonation States of Dipeptides Probed by Polarized Raman, UV–Resonance Raman, and FTIR Spectroscopy

5 AUTHORS, INCLUDING:

Reinhard Schweitzer-Stenner
Drexel University
219 PUBLICATIONS **4,368** CITATIONS

SEE PROFILE

Vasil Pajcini
Evans Analytical Group
11 PUBLICATIONS **271** CITATIONS

SEE PROFILE

Sanford A Asher
University of Pittsburgh
312 PUBLICATIONS **13,097** CITATIONS

SEE PROFILE

Different Conformers and Protonation States of Dipeptides Probed by Polarized Raman, UV−Resonance Raman, and FTIR Spectroscopy

Guido Sieler,[†] Reinhard Schweitzer-Stenner,*,[†] Janet S. W. Holtz,[‡] Vasil Pajcini,[‡] and Sanford A. Asher[‡]

FB1-Institut für Experimentelle Physik, Universität Bremen, 28359 Bremen, Germany, and Department of Chemistry, University of Pittsburgh, Pittsburgh, Pennsylvania 15260

We have measured the polarized nonresonance and resonance Raman as well as FTIR spectra of the model peptides glycylglycine and *N*-acetylglycine in H_2O and D_2O at pH/pD values between 1.5 and 12.0 with visible, near UV, and far UV excitation wavelengths. The spectra were self-consistently analyzed to obtain reliable spectral parameters of even strongly overlapping bands. Additionally, we have analyzed the polarized nonresonance and preresonance Raman spectra of glycylglycine single crystals. The most important result of this analysis is that for glycylglycine all amide bands as well as the symmetric carboxyl stretch band at ca. 1400 cm^{-1} are doublets. As shown in an earlier study (Sieler, G.; Schweitzer-Stenner, R. *J. Am. Chem. Soc.* **1997**, *119*, 1720) the amide I doublet results from vibrational coupling of the delocalized H_2O bending mode with internal coordinates of the amide I mode. The amide III doublet is interpreted to result from vibrational coupling between the twisting mode of the C_α methylene group and internal coordinates which normally give rise to the amide III vibration (i.e., CN and $C_{\alpha 1}$C stretching). In contrast, the amide II and carboxylate subbands are assigned to different conformers with respect to the torsional coordinate of the carboxylate group. While the higher frequency subband of the amide II and carboxylate bands may reflect a parallel orientation of the latter with respect to the peptide, which could be stabilized by hydrogen bonding to NH, the lower frequency band may reflect different orientations in which the carboxylate is hydrogen bonded to water. For *N*-acetylglycine we also observe two subbands underlying amide I and the carboxyl symmetric stretch band, which again reflects vibrational mixing with water and multiple rotational substates of the carboxylate, respectively.

Introduction

The simplest molecule containing a single peptide group which can serve as a model for investigating the amide linkage in proteins and peptides is *N*-methylacetamide (NMA, Figure 1). Numerous spectroscopic studies have examined its vibrational dynamics,[1] but a detailed understanding of this simple molecule only recently emerged by combining UV−Raman, visible, and FT-Raman as well as FTIR spectroscopies with a normal coordinate analysis based on force constants obtained from ab initio calculations.[2,3] These studies revealed that the amide II frequency depends significantly on the orientation of the methyl group attached to the peptide nitrogen.[2b,3c] Even more important, a thorough spectral analysis and normal coordinate calculations on NMA−$(H_2O)_2$ complexes revealed that the amide I band of aqueous NMA is a doublet due to vibrational mixing between this mode and the bending mode of surrounding water molecules.[2a,b] Finally, the above studies revealed that the electronic transition from the highest occupied amide π orbital into the lowest occupied π* orbital involves bond length changes, not only of the carbonyl and CN bonds but also for the adjacent CC and NC bonds. This shows that the π → π* transition is much more delocalized than earlier anticipated. The advantage of using NMA as a model peptide stems to a significant extent from the fact that it does not contain any charged groups. Thus, however, NMA is of limited use for many peptides because Coulomb interactions between charged terminal groups significantly affect the structure as well as the dynamics of small peptides containing up to five amino acids.[4] Simple dipeptides such as glycylglycine (DGL: diglycine, Figure 1), which are zwitterions at physiological pH, are ideal model systems for exploring the influence of negatively and positively charged groups on the peptide's vibrational dynamics as well as on its electronic and structural properties. A variety of techniques have been employed so far to characterize the ground-state structure of dipeptides. X-ray and neutron diffraction data have shown that their carboxylate and amide planes are not parallel.[5] The angle between them, however, strongly depends on the crystal structure. Hence, these crystallographic data are of limited use for determining the solution structure of small peptides. NMR studies on the dipeptide isomers glycyl-L-alanine and L-alanylglycine by Beeson and Dix utilized methylene proton resonance to obtain conformational information.[6] Their results led them to suggest that the Coulomb interaction between the terminal groups favors rotamers in which the NH_3^+−carboxylate distance is minimized. The authors also performed molecular mechanics calculations based on a CHARMM force field, which yielded seven different rotamers with similar ground-state energies. While some of them meet the requirements for maximal Coulomb interactions between the terminal groups, the lowest energy conformer was a rotamer with a larger end to end distance. Thus, the role of electrostatic interactions in determining the structure of dipeptides remains unresolved.

* To whom all correspondence should be addressed. Phone: **49-421-218-2509. Fax: **49-421-218-7318. E-mail: stenner@theo.physik.uni-bremen.de.
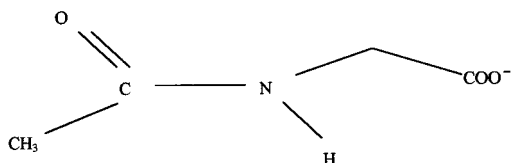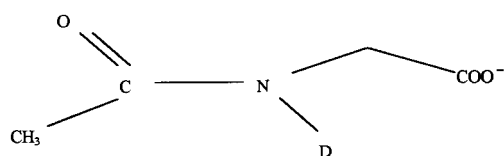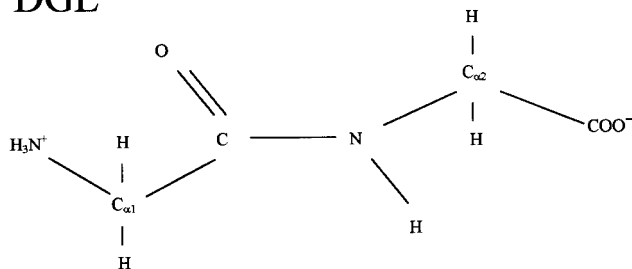† Universität Bremen.
‡ University of Pittsburgh.
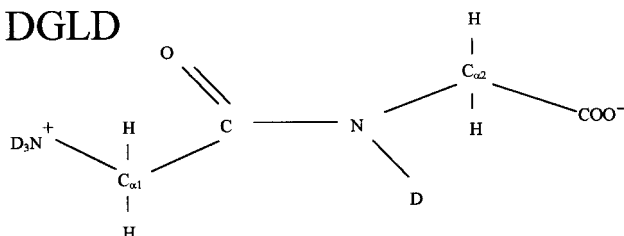
NMA
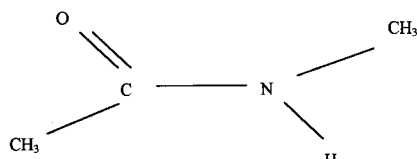
AGL

AGLD

DGL

DGLD

Figure 1. Steric conformations of the model peptides NMA, AGL, AGLD, DGL, and DGLD.

Most recent UV—Raman studies on DGL and similar dipeptides have provided some detailed information on their excited electronic states.[7] Chen et al.,[7a] for instance, identified a charge-transfer transition from the nonbonding carboxylate n_{COO} into the antibonding amide-like π^* orbital ($n_{COO} \rightarrow \pi_a^*$, CT_n). Several lines of evidence were provided to show that the prominent amide modes, as well as the symmetric carboxylate stretch, are vibronically coupled to this electronic transition, thus giving rise to resonance enhancement at 200 nm excitation. In a subsequent study on a novel crystal of hydrated DGL, Pajcini et al.[7b] measured the Raman tensor of these modes to determine the direction of the transition dipole for the above charge transfer as well as for the lowest intrapeptide $\pi_a \rightarrow \pi_a^*$ (NV₁) transition.

Little spectroscopically determined information exists on the vibrational dynamics of dipeptides in aqueous solution. The UV—Raman study by Chen et al.[7a] identified and assigned those

Raman bands that are strongly enhanced in the far UV. A complete and accurate normal-mode analysis, however, requires the identification, characterization, and assignment of all bands in the visible nonresonance Raman and IR spectra. To our knowledge this has not yet been accomplished. Most recent normal mode calculations on DGL—hydrochloride based on quantum mechanically determined force fields[8] were compared with earlier (unpolarized) Raman spectra of crystallized DGL[9] and the IR spectra of dried DGL. However, these substances do not provide an appropriate basis for a spectroscopically determined force field, because peptides are in close proximity in the solid state so that the vibrational frequencies are significantly influenced by transition dipole coupling between vibrations of nearest neighbors.[1c] Moreover, the structure in the solid may be different from that preferred in an aqueous environment.

As a first step toward a comprehensive vibrational analysis of small zwitterionic peptides, recent work from our laboratory has provided evidence through spectral decomposition that the amide I band of DGL and *N*-acetylglycine (AGL, Figure 1) in aqueous solution is composed of two broad subbands (DGL, 1675 (AI₁) and 1692 (AI₂) cm⁻¹; AGL, 1627 (AI₁) and 1648 (AI₂) cm⁻¹), which show slightly different depolarization ratios.[10] This finding parallels earlier results on NMA in water and is interpreted as resulting from mixing between internal peptide coordinates and delocalized bending motions of the sourrounding water molecules. In the present study we extend this type of investigation to the entire frequency region between 800 and 1800 cm⁻¹ of DGL and AGL in H_2O and D_2O (DGLD and AGLD). Moreover, we have measured and analyzed the pH dependence of the spectra from aqueous DGL between pH 1.5 and 12.0, and also of AGL between pH 1.5 and 6.0 to explore the influence of the terminal charges on structure and vibrational dynamics. A self-consistent global fitting enabled us to identify and subsequently assign even strongly overlapping bands. Thus, we also obtained information about coexisting conformers and their dependence on pH. As in earlier studies from this and other laboratories, the depolarization ratios were utilized to identify electronic transitions to which the corresponding modes are vibronically coupled.[2a,b,7a] Finally, we compare UV—resonance Raman spectra of DGL in solution and in a single crystal to assess the subbands underlying the band profiles of amide II, III, and the COO⁻ₛₛ.

Theoretical Background

In this study we utilize the depolarization ratio of Raman bands to infer the electronic transitions to which the corresponding vibrations are vibronically coupled. In the following we outline the basic concept of this strategy.

Provided that the exciting laser beam is polarized perpendicular to the scattering plane, the depolarization ratio of non resonance Raman bands for statistically oriented molecules is written as[11a]

$$\rho = \frac{I_y}{I_x} = \frac{3\gamma^2}{45\alpha^2 + 4\gamma^2} \tag{1}$$

where α^2 and γ^2 are the tensor invariants reflecting isotropic and anisotropic scattering, respectively. I_x and I_y denote the intensities of the scattered light polarized parallel (x) and perpendicular (y) to the polarization of the exciting laser beam. The Raman tensor is symmetric and the laboratory coordinate system can therefore be rotated to yield the three principal axes

of the Raman tensor (designated as PART by Pajcini et al.[7b]). Hence we can neglect off-diagonal elements in the following.

Let us now assume that a molecular vibration gains its Raman intensity from Franck−Condon type vibronic coupling to a single nondegenerate electronic transition. In this case one axis of the Raman tensor coincides with the direction of its electric dipole moment (MART: major axis of the Raman tensor in the diagonal frame). A simple calculation shows that this causes a depolarization ratio of 0.33 for all excitation wavelengths.[11a]

The situation becomes more complicated if two electronic transitions are involved that are oriented by an angle ϕ with respect to each other. This is the case for most of the Raman active modes investigated in this study, which are coupled to an intrapeptide and a carboxylate−peptide charge-transfer transition. By a tedious calculation[7a] one can show that in this case the Raman tensor contains two elements, α_{xx} and α_{yy}. Thus, the depolarization ratio can be written as[12]

$$\rho = \frac{1 + 3\delta^2}{8 + 4\delta^2} \qquad (2)$$

with

$$\delta = \frac{|\alpha_{xx} - \alpha_{yy}|}{|\alpha_{xx} + \alpha_{yy}|} \qquad (3)$$

If the displacement ΔQ of the corresponding excited state along the normal coordinate Q is positive or negative for both transitions, it follows that with preresonance excitation the corresponding PART elements have the same sign. In this case the depolarization ratio may vary between 0.125 and 0.33, depending on the relative magnitude of the tensor elements. In contrast, if ΔQ exhibits an opposite sign for the two transitions, the depolarization ratio varies between 0.33 and 0.75.

In the case that a vibration is coupled to three electronic transitions with noncoplanar transition dipole moments, one obtains three PART elements. In the simplest case where all these elements exhibit identical signs the depolarization ratio varies between 0 and 0.33.

Materials and Methods

Material. Glycylglycine and *N*-acetylglycine were commercially obtained from Sigma Chemical Co. and dissolved in H_2O and D_2O without further purification. For all experiments the DGL and AGL concentrations were adjusted to 1.0 and 0.4 M for the nonresonance and 8 mM for the resonance Raman experiments, respectively. The solvent contained $NaClO_4$ (DGL, 0.25 M; AGL, 0.1 M) whose 934 cm^{-1} Raman band was used as an internal standard.

To ensure an identical concentration at all pH values, we prepared two stock solutions with pH 1.5 and 12.0 for DGL and pH 1.5 and 6.0 for AGL samples. Their pH was adjusted by adding HCl or NaOH to H_2O, and DCl and NaOD to the D_2O solutions. The pD values were determined by using the method of Glasoe and Long[13] to correct the values obtained from pH electrode measurements. The pH/pD values were adjusted by mixing the corresponding stock solutions and ranged between pH 1.5 and 12.0 for DGL and pH 1.5 and 6.0 for AGL.

Instrumentation. The instrumentation used for the non resonance Raman experiments is described in detail elsewhere.[10,14] Briefly, most of the non resonance Raman spectra reported in this study were recorded with continuous wave (cw) excitation (363.8 nm) provided by an argon ion laser (Spectra Physics, 2020-05). The Raman scattered light was collected in

TABLE 1: Intensity Ratio of the ClO$_4^-$ and the 1640 cm^{-1} H$_2$O Band and the Depolarization Ratio of the Latter as Measured at Two pH Values Reflecting the Acid and Basic Boundary of the pH Range Used in This Study

pH	$I_{x,ClO_4^-}/I_{x,H_2O}$	ρ_{H_2O}
1.5	1.36	0.47
13.0	1.28	0.42

a backscattering geometry. The spectral resolution was about 4 cm^{-1} at the employed excitation wavelength. Some of the nonresonance spectra were recorded using a excimer pumped dye laser and an experimental setup described by Unger et al.[14] All Raman spectra were measured polarized parallel (x) and perpendicular (y) to the polarization of the exciting laser beam.

UV−resonance Raman spectra of DGL in solution and DGL single crystals were obtained as described earlier.[7]

Spectral Analysis. All spectra were analyzed by a recently developed program MULTIFIT.[14] All spectra shown in this paper are normalized to the internal standard, i.e., the ClO$_4^-$ band at 934 cm^{-1}. To eliminate the broad depolarized H_2O Raman band at 1640 cm^{-1}, we measured the solvent's reference spectra for both polarizations, which were then subtracted from the corresponding peptide spectra. The intensity ratio of the ClO$_4^-$ and the 1640 cm^{-1} H_2O band were found to be pH independent (Table 1), so that the former can be used as the internal standard for all spectra observed. The intensities of the normalized polarized Raman bands were derived from their band areas and used to calculate the depolarization ratio.

To eliminate ambiguities in the fits to the experimentally observed spectra, we have performed a global self-consistent analysis in that we simultaneously fitted spectra taken with different excitation wavelengths between 360 and 530 nm for both polarizations as well as corresponding FTIR spectra with identical frequency positions, band shapes, and half-widths. The quality and the statistical significance of the fits were judged by their residuals and reduced χ_R^2 numbers.[15] Further details are given in the Supporting Information.

The Raman spectra of DGL and AGL at pH = 1.5 and pH = 12.0 were separately fitted, since some Raman bands exhibit frequency shifts due to the protonation/deprotonation states of the terminal groups. The UV−resonance Raman spectra of DGL were fitted with the spectral parameters obtained from the nonresonance and IR data. All these band profiles had to be convoluted with the spectrometer function, which was reasonably well approximated by a Gaussian of 10 cm^{-1} width.[16]

Results

Spectral Analysis and Assignment. We have measured the polarized Raman spectra of DGL, DGLD, AGL, and AGLD taken between 800 and 1800 cm^{-1} with 363 nm excitation at neutral pH/pD (Figure S1). The corresponding FTIR spectra of the above substances are depicted in Figure S2. Moreover, we measured the resonance Raman spectra of DGL in aqueous solution (pH 5.7) with 206 nm excitation (Figure S3) and the polarized Raman spectra of DGL single crystals with 488 and 244 nm (Figure S4).[7b] The spectral parameters were obtained by the self-consistent analysis of the above spectra. The frequency positions, half-widths, and depolarization ratios of all explicitly discussed bands are listed in Tables 2 and 3, whereas a complete list of all bands obtained are given in Tables S1−S4. The DGL single crystal spectra taken with 488 nm excitation were consistently fitted with a model considering only Lorentzian band shapes, in accordance with the expectation that inhomogeneous broadening should be absent.

Dipeptides Probed by Raman Spectroscopy

J. Phys. Chem. B, Vol. 103, No. 2, 1999 **375**

TABLE 2: Spectral Parameters, i.e., Frequency ν, Half-Widths Γ (L, Lorentzian; G, Gaussian; Corrected for the Spectrometer Function) Derived from the Self-Consistent Analysis of the DGL and DGLD Raman Spectra[a]

mode	ν (cm^{-1})	Γ_L (cm^{-1})	Γ_G (cm^{-1})	$\chi_{r,x-pol}^2$	$\chi_{r,y-pol}^2$	ρ_{363}
			DGL			
$C_{\alpha2}H_{2t}$	1257.99	3.03	19.68	0.8	0.5	0.13
A III$_1$	1277.09	9.81	23.16			0.26
A III$_2$	1285.82	17.11	17.91			0.11
$C_{\alpha2}H_{2w}$	1319.09	14.39	9.63			0.56
COO$^-_{ss1}$	1394.40	10.8	10.1	1.55	1.33	0.57
COO$^-_{ss2}$	1407.99	14.75				0.28
$C_{\alpha2}H_{2b}$	1427.37	7.13	9.99			0.31
$C_{\alpha1}H_{2b}$	1444.34	3.53	12.00			0.65
A II$_1$	1560.97	47.44		1.26	1.1	0.12
A II$_2$	1583.75	27.29				0.36
COO$^-_{as}$	1602.50	25.47	16.9			0.63
NH$_3^+{}_{ab}$	1636.28	58.64				0.34
A I$_1$	1675.10	14.60	24.00			0.14
A I$_2$	1692.00	11.81	19.96			0.18
			DGLD			
$C_{\alpha2}H_{2t}$	1257.56	39.35		1.95	1.41	0.54
$C_{\alpha1}H_{2t}$	1274.22	5.80	23.65			0.73
$C_{\alpha2}H_{2w}$	1314.92	15.66				0.18
$C_{\alpha2}H_{2w}$ + COO^-_b	1363.52		18.91	2.05	1.85	0.36
COO$^-_{ss1}$	1395.42	4.55	15.21			0.49
COO$^-_{ss2}$	1408.88		13.94			0.29
$C_{\alpha2}H_{2b}$	1426.41	7.08	9.14			0.35
$C_{\alpha1}H_{2b}$	1442.46	3.53	12.30			0.43
A II'	1489.93	11.46	14.35			0.18
COO$^-_{as}$	1596.12	25.47	16.90	1.33	1.29	0.61
A I'	1674.31	11.74	21.13			0.14

[a] The reduced χ_r^2 values refer to the frequency regions indicated in the table. The depolarization ratio ρ was determined at 363 nm.

TABLE 3: Spectral Parameters, i.e., Frequency ν, Half-Widths Γ (L, Lorentzian; G, Gaussian; Corrected for the Spectrometer Function) Derived from the Self-Consistent Analysis of the AGL and AGLD Raman Spectra[a]

mode	ν (cm^{-1})	Γ_L (cm^{-1})	Γ_G (cm^{-1})	$\chi_{r,x-pol}^2$	$\chi_{r,y-pol}^2$	ρ_{363}
			AGL			
CH$_{2t}$	1265.97	13.21	21.14	1.27	1.82	0.22
A III	1298.86	9.78	16.05			0.21
CH$_{2w}$	1325.42	13.03	5.59			0.67
CCH$_{3sb}$	1380.00	10.73	6.79	2.1	1.32	0.39
COO$^-_{ss1}$	1394.73		20.33			0.63
COO$^-_{ss2}$	1406.54	5.01	11.92			0.39
CH$_{2b}$	1424.79	19.14	3.16			0.33
CCH$_{3ab}$	1445.88	21.89				0.48
A II	1568.06	63.35		1.10	0.82	0.16
COO$^-_{as}$	1600.36	25.50	33.45			0.75
A I$_1$	1627.37	33.62	28.19			0.17
A I$_2$	1648.19	7.83	40.16			0.22

mode	ν (cm^{-1})	Γ_L (cm^{-1})	Γ_G (cm^{-1})	$\chi_{r,x-pol}^2$	$\chi_{r,y-pol}^2$	ρ_{413}
			AGLD			
CH$_{2t}$	1272.58	16.92		1.21	2.30	0.66
CH$_{2w}$	1314.35	15.94				0.22
CCH$_{3sb}$	1371.18	9.70		1.37	1.75	0.75
COO$^-_{ss1}$	1393.71	8.45	11.04			0.50
COO$^-_{ss1}$	1406.43		11.16			0.23
CH$_{2sb}$	1425.89	21.58				0.52
CCH$_{3ab}$	1441.69	12.95				0.63
A II'	1494.04	16.56	6.17			0.13
COO$^-_{as}$	1594.50	44.77	4.31	1.62	1.93	
A I'	1629.07	28.62	4.91			0.15

[a] The reduced χ_r^2 values refer to the frequency regions indicated in the table. The depolarization ratio ρ was determined at 363 nm for AGL and 413 nm for AGLD.

In the following we elucidate details emerging from this analysis for different sections of the spectra. Assignments are made on the basis of normal coordinate analyses for glycine, alanine, and crystallized triglycine (Glyglygly, TGL).[17a−f] Additionally, we took into account the band assignments of dialanine (AlaAla) Raman and VCD spectra carried out by Diem and co-workers.[17a]

(a) 1500−1800 cm^{-1}. Figure 2 shows the spectral decomposition of the polarized Raman as well as of the FTIR spectra of DGL and DGLD measured between 1500 and 1800 cm^{-1}. As mentioned in our earlier study, amide I of DGL appears as a doublet with Voigtian subbands at 1675 (AI$_1$) and 1692 cm^{-1} (AI$_2$), while amide I' of DGLD is a single band at 1674 cm^{-1}. This and the analysis of Raman spectra from DGL in H$_2$O/D$_2$O mixtures led us to conclude that the amide I doublet arises from vibrational mixing between internal coordinates contributing to the eigenvector of amide I and the bending modes of water molecules constituting the peptide's aqueous environment.[10]

Appropriate fitting to the Raman and IR spectra of DGL requires consideration of another broad Gaussian band at 1636 cm^{-1}, which is absent in the DGLD spectra. This band may in fact consist of multiple unresolved subbands. Comparison with normal coordinates calculated for glycine,[17b,d,e] alanine,[17f] DGL−hydrochloride,[8] and TGL[17b] and its absence in the spectra of DGLD strongly indicates that it results from the NH$_3^+$ asymmetric bending modes (NH$_{3ab}$) of the ammonium ion. In an undistorted local symmetry this mode is 2-fold degenerate, but any type of asymmetric environment causes splitting into an in-plane and an out-of-plane component.[17b] This may be the reason, for the spectral broadening observed in our spectra. For some reason, which we presently do not understand, the

corresponding band is weak in the spectra of DGL crystals, where it only appears in the *xy* spectrum taken at 488 nm (Figure S4).

In the spectra of the single crystal the amide I appears as doublet with subbands at 1624 and 1665 cm^{-1} (cf. Figure S4 and ref 7b). This splitting is much larger than that observed in the Raman spectra of polycrystalline NMA[18] but comparable with that observed for other crystal structures.[9] Moreover, its average frequency (i.e., 1645 cm^{-1}) appears at a much lower frequency than the peak position observed for DGL in solution (Figure S1, 2). All these findings are discussed in more detail below.

The amide II band of DGL appears comparatively weak and broad in the nonresonance Raman spectra, but quite strong and asymmetric in the IR spectrum. The minimal model to which all these spectra could be simultaneously fit comprises two Gaussian amide II subbands at 1560 cm^{-1} (AII$_1$) and 1584 cm^{-1} (AII$_2$). While AII$_1$ is more intense in the near UV−Raman as well as in resonance Raman spectra (Figure S3), both subbands are of comparable intensity in the IR spectrum. In contrast, amide II' of all DGLD spectra can be fit by a single band. This parallels observations recently made for NMA, for which the amide II doublet was assigned to two conformers with different methyl orientations.[2b] As we will make plausible below, the amide II subbands of DGL are likely to reflect different conformations of the carboxylate group with respect to its torsional coordinate. The conformational origin of the amide II doublet is underscored by the observation that amide II appears as a single band in all the visible and UV−Raman spectra of the DGL crystal (Figure S4).

The IR spectrum of DGLD displays a strong isolated Voigtian band at 1596 cm^{-1}. It also appears as a depolarized band in the
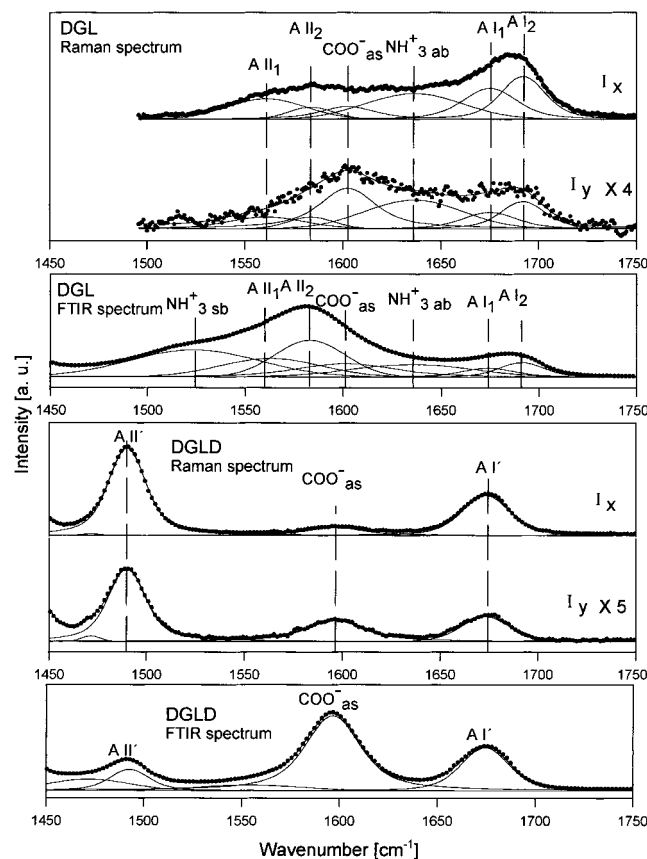
Figure 2. Spectral decomposition of the parallel (*x*) and perpendicular (*y*) polarized DGL ($\lambda = 526$ nm) and DGLD ($\lambda = 384$ nm) spectra at neutral pH/pD recorded between ca. 1500 and 1750 cm^{-1}. The dotted lines represent the experimentally observed spectra; the solid lines result from the fit to the data. Additionally, the fits to the FTIR spectra of these compounds are shown for the respective spectral window.
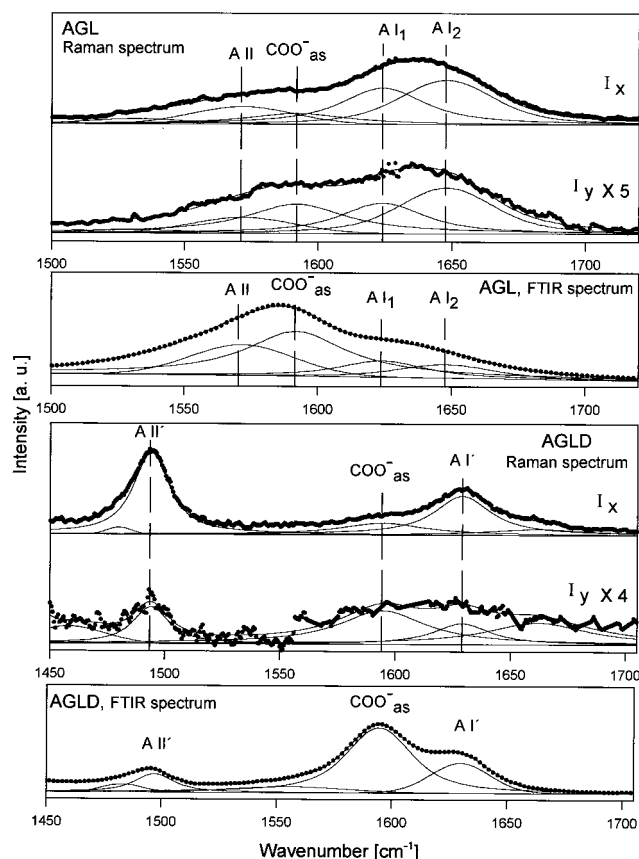
Figure 3. Spectral decomposition of the parallel (*x*) and perpendicular (*y*) polarized AGL ($\lambda = 407$ nm) and AGLD ($\lambda = 413$ nm) spectra at neutral pH/pD recorded between ca. 1500 and 1750 cm^{-1}. The dotted lines represent the experimentally observed spectra; the solid lines result from the fit to the data. Additionally, the fits to the FTIR spectra of these compounds are shown for the respective spectral window.

Raman spectrum, though less dominant. The corresponding band in DGL is slightly shifted to higher frequencies. It overlaps with the amide II band and contributes to its apparent noncoincidence between the peak frequencies in the parallel and perpendicular polarized spectrum. As shown later, this band disappears upon carboxylate protonation at acidic pH. This and a comparison with the normal coordinates of other peptides[8,17a−c] lead us to assign it to the antisymmetric carboxylate stretch (COO$_{as}$).

Additionally, the IR spectrum of DGL shows a broad band at 1530 cm^{-1}, which appears as a shoulder of amide II. It is absent in the Raman spectra and disappears in the IR upon deuteration of the NH bonds. The only possible candidate for this band is the NH$_3^+$$_{sb}$,[8b,17f] even though it is surprising that it is absent in the visible and UV−Raman spectra while it appears in the visible Raman spectra of the DGL α-crystal.

Figure 3 depicts the corresponding Raman and IR spectra of AGL and AGLD. Compared with its position in the DGL spectra, the amide I peak frequency is significantly downshifted, i.e., from 1689 to around 1635 cm^{-1}. This shows the strong influence of the positively charged ammonium ion on this mode's ground state frequency. The broad amide I band greatly overlaps the amide II and the COO$_{as}$ bands in the perpendicular polarized Raman and IR spectrum. The corresponding spectra of AGLD are less complicated and contain only the smaller amide I′ and the COO$_{as}$ band. A self-consistent fitting to all these spectra yields two amide I subbands for AGL at 1627 and 1648 cm^{-1}, which for AGLD merge into a single band at 1629 cm^{-1}. This result is nearly identical to that recently obtained for NMA in H$_2$O and D$_2$O and is again attributed to

vibrational mixing between amide I components and the bending mode of surrounding water molecules.[2a,b]

In contrast to the results obtained for DGL and aqueous NMA, the amide II band of AGL can be fitted by a single Gaussian band at 1567 cm^{-1}. This is also the case for an AGL spectrum taken with 206 nm excitation (data not shown). Again, this band is weak in the visible Raman and in the IR spectrum, but comparatively strong in the IR spectrum.

The absence of discernible subbands suggests the presence of only one conformer. However, the large Gaussian half-width reflects conformational heterogeneity due to several subconformations that cannot be distinguished spectroscopically. In contrast, amide II′ of AGLD is Voigtian (at 1494 cm^{-1}) and has a much smaller halfwidth. This underscores the notion that amide II′ is less sensitive to conformation than amide II.

Except for the COO$_{as}$ band, all bands appear nearly polarized (i.e., $0 < \rho < 0.33$) in all spectra discussed above. Their depolarization ratio rather suggests vibronic coupling to several electronic transitions in the far UV, i.e., the intrapeptide NV$_1$ transition, the CT$_n$ transition from the carboxylate to the lowest π^*-orbital of the peptide (for amide II), and the intrinsic carbonyl transition NV$_2$ (for amide I). This is discussed in more detail below.

(b) 1350−1500 cm^{-1}. Figure 4 exhibits the polarized Raman and the FTIR spectra of DGL and DGLD between 1350 and 1500 cm^{-1}. The corresponding spectra of AGL and AGLD are shown in Figure 5.

For all substances this spectral region is dominated by a nearly depolarized band ($\rho = 0.5$) at 1394 cm^{-1}. Its frequency remains
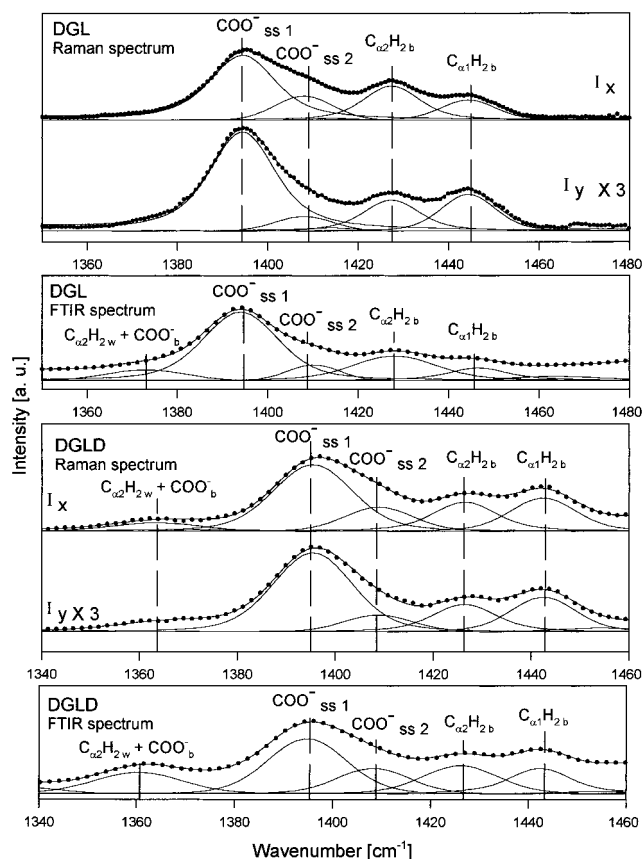
Dipeptides Probed by Raman Spectroscopy

J. Phys. Chem. B, Vol. 103, No. 2, 1999 **377**

Figure 4. Spectral decomposition of the parallel (*x*) and perpendicular (*y*) polarized DGL ($\lambda = 526$ nm) and DGLD ($\lambda = 384$ nm) spectra at neutral pH/pD recorded between ca. 1350 and 1500 cm^{-1}. The dotted lines represent the experimentally observed spectra; the solid lines result from the fit to the data. Additionally, the fits to the FTIR spectra of these compounds are shown for the respective spectral window.

Figure 5. Spectral decomposition of the parallel (*x*) and perpendicular (*y*) polarized AGL ($\lambda = 407$ nm) and AGLD ($\lambda = 413$ nm) spectra at neutral pH/pD recorded between ca. 1350 and 1500 cm^{-1}. The dotted lines represent the experimentally observed spectra; the solid lines result from the fit to the data. Additionally, the fits to the FTIR spectra of these compounds are shown for the respective spectral window.

nearly unchanged upon NH $\leftrightarrow$ ND exchange. It clearly overlaps a polarized sideband ($\rho = 0.28$) at 1408 cm^{-1}, which is also unaffected by deuteration. As we will see below, however, both bands disappear upon carboxylate protonation.

Asher and co-workers have recently identified a relatively strong COO$^-_{ss}$ band in the UV−Raman spectra of AGL and DGL,[7] which gains resonance enhancement from the above-mentioned CT-transition as well as from the intrinsic carboxylate $\pi_{COO} \rightarrow \pi_{COO}{}^*$ transition. The present data suggest that the COO$_{ss}$ band appears as a doublet (COO$^-_{ss1}$ and COO$^-_{ss2}$, cf. Tables 2 and 3). Both subbands appear also in the UV−resonance spectrum (Figure S3). In contrast, the Raman spectra of the DGL crystal (Figure S4) exhibit only a single COO$^-_{ss}$ band at 1404 cm^{-1}.

In a previous study Chen et al.[7a] suggested that the COO$^-_{ss}$ bands of AGL and DGL are overlapped by Raman bands resulting from CH$_{3sb}$ and C$_{\alpha 1}$H$_{2b}$ modes, since their UV−resonance Raman spectra of DGL and AGL at pH 1.5 still show Raman bands at 1395 and 1380 cm^{-1}, respectively. However, these bands cannot be related to the polarized band at 1407/1408 cm^{-1} for the following reasons. For AGL, the CH$_{3sb}$ band can be observed as a shoulder at 1380 cm^{-1} in the near UV Raman spectra (Figures S1 and 5). Its spectral parameters were determined with high accuracy. The CH$_{3sb}$ band is relatively intense and exhibits a depolarization ratio of about 0.39, which is somewhat higher than the value obtained for the Raman band of the corresponding C(C)H$_{3sb}$ mode of NMA.[2b] Its appearance in the UV−resonance spectrum of AGL suggests that it gets its intensity from vibronic coupling to the peptide NV$_1$ transition,
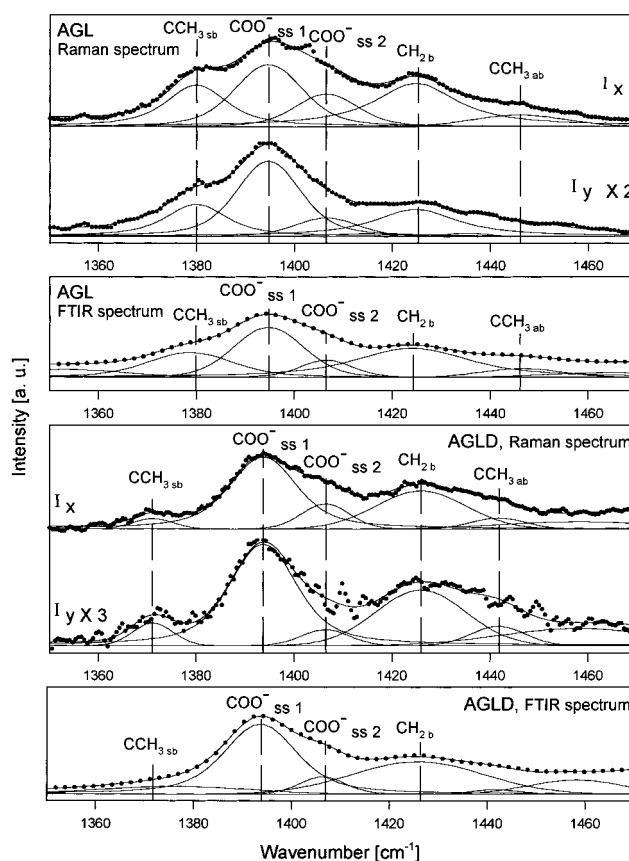
because its eigenvector contains a significant contribution from CC$_s$.[2a,c] As shown below, for DGL we also observed a comparatively strong band at 1400 cm^{-1} in the UV−resonance Raman spectrum measured at pH 1.5. In the near UV−Raman and in the visible Raman spectra measured at the same pH, however, this (polarized) band is less intense. In the corresponding spectra of DGLD (pD = 1.5) this band is depolarized and weak, while the band at 1408 cm^{-1} appears nearly unaffected by the NH $\leftrightarrow$ ND exchange at neutral pH. Hence, we conclude, that the 1400 cm^{-1} band does not significantly contribute to the near UV−Raman spectra of the zwitterionic molecule and is therefore not related to the 1408 cm^{-1} band. In the UV−resonance Raman and in the IR spectra of the zwitterionic state (Figures S2 and S3) the band is identified at 1385 cm^{-1}.

Comparison with the normal coordinates of glycine[17b] and TGL[17a,c] suggests that the above band at 1385 cm^{-1} is assignable to C$_{\alpha 1}$H$_{2w}$ rather than to C$_{\alpha 1}$H$_{2b}$, as earlier suggested.[7a] The latter is related to the depolarized band at 1444 cm^{-1}.

The two DGL bands at 1427 and 1444 cm^{-1} result from C$_{\alpha 2}$H$_{2b}$ and C$_{\alpha 1}$H$_{2b}$, respectively. The assignment to methylene bending modes clearly follows from the normal coordinates of glycine,[17b] alanine,[17f] and TGL.[17a,c] The 1444 cm^{-1} band is absent in the AGL spectra, and is replaced by a broader depolarized band arising from the antisymmetric methyl bending mode.[2b] Hence, the former must arise from the N-terminal methylene group. While the C$_{\alpha 2}$H$_{2b}$ band is polarized with a depolarization ratio close to 0.33, the C$_{\alpha 1}$H$_{2b}$-band appears nearly depolarized. This indicates that the Raman cross section
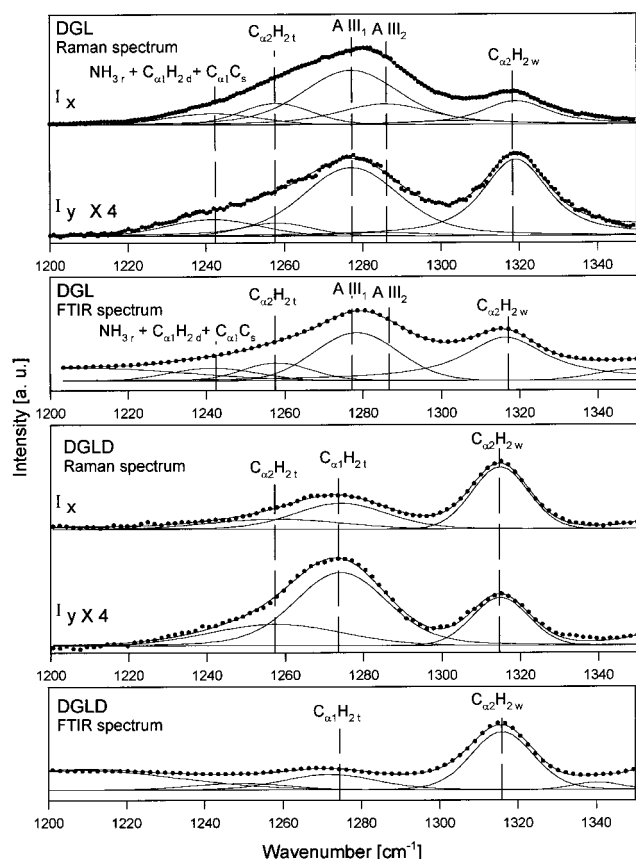
Figure 6. Spectral decomposition of the parallel (*x*) and perpendicular (*y*) polarized DGL ($\lambda = 526$ nm) and DGLD ($\lambda = 384$ nm) spectra at neutral pH/pD recorded between 1200 and 1350 cm^{-1}. The dotted lines represent the experimentally observed spectra; the solid lines result from the fit to the data. Additionally, the fits to the FTIR spectra of these compounds are shown for the respective spectral window.
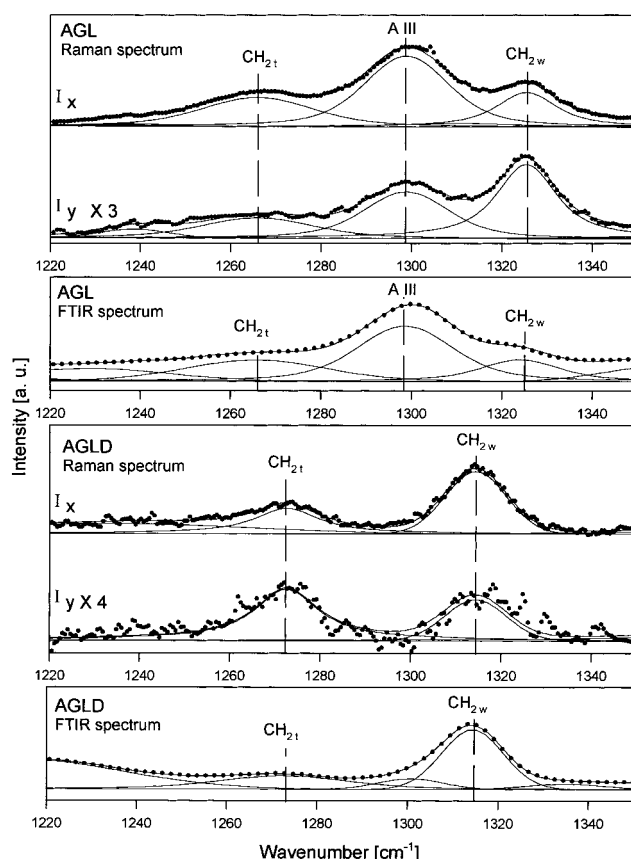
Figure 7. Spectral decomposition of the parallel (*x*) and perpendicular (*y*) polarized AGL ($\lambda = 407$ nm) and AGLD ($\lambda = 413$ nm) spectra at neutral pH/pD recorded between ca. 1200 and 1350 cm^{-1}. The dotted lines represent the experimentally observed spectra; the solid lines result from the fit to the data. Additionally, the fits to the FTIR spectra of these compounds are shown for the respective spectral window.

of $C_{\alpha 2}H_{2b}$, predominantly arises from Franck–Condon coupling to a single electronic transition. It should be mentioned that the above assignment disagrees with results from a recent normal coordinate analysis on isolated glycylglycine–hydrochloride,[8b] which predicts that the C-terminal methylene deformation modes occur at higher frequencies compared to their N-terminal counterparts. In agreement with earlier calculations by Krimm and associates,[17e] our data show that this is not the case (cf. also the assignment of the wagging and twisting modes in the next section).

(c) 1200–1350 cm^{-1}. Figures 6 and 7 exhibit the Raman and IR spectra of DGL, DGLD, AGL, and AGLD measured between 1200 and 1350 cm^{-1}. The spectra of DGL display two broad bands centered at 1280 and 1319 cm^{-1}. The former is clearly asymmetric and can be decomposed into four polarized bands at 1242, 1258, 1277, and 1286 cm^{-1}. In DGLD they are replaced by a broad, asymmetric, and totally depolarized band, which is composed of two bands at 1258 and 1274 cm^{-1}, whereas the band at 1319 cm^{-1} becomes more polarized and is slightly downshifted to 1315 cm^{-1}. Again, we utilize the normal coordinates of other peptides[17c] and amino acids[17e,f] to assign the above bands. The weak band at 1242 cm^{-1} is attributed to a mixture of NH_{3r} (r: rocking), methylene deformation, and $C_{\alpha 2}C_s$.[17f] The band at 1258 cm^{-1} appears polarized ($\rho = 0.13$) in the spectra of DGL, while it is depolarized for DGLD. It is assigned to $C_{\alpha 2}H_{2t}$ (twisting). In DGL this mode gets admixed to some amide and carboxylate coordinates to yield a drastic decrease of its depolarization ratio ($0.75 \rightarrow 0.13$). The DGLD band at 1274 cm^{-1} is attributed to $C_{\alpha 1}H_{2t}$.

The assignment of the two remaining DGL bands at 1277 and 1286 cm^{-1} is less straightforward. This doublet cannot arise from the above conformers, since it also exists in the spectra of the single crystal (Figure S4). The excitation wavelength dependence of the relative intensities suggests that the 1277 cm^{-1} band is amide III while the 1286 cm^{-1} band arises from $C_{\alpha 1}H_{2t}$ mixed with $C_{\alpha 1}C_s$ and even CN_s so that it gets some enhancement by weak coupling to the NV_1 and CT_n transitions. This notion is supported by the observation that the 1277 cm^{-1} band is strongly enhanced with 206 nm excitation (Figure S3); i.e., the intensity ratio I_{1277}/I_{1286} increases from 2.4 at 362 nm to 5.3 at 206 nm. Other data, however, argue against such a clear assignment. The higher frequency band becomes predominant for the fully protonated state and relatively more intense in the fully deprotonated state, so that both bands appear as suitable candidates for amide III (Figure 8). The corresponding band profiles in the 244 nm spectra are less asymmetric, but a consistent fitting to all bands still requires at least two subbands (Figure 9). Taken together, our data indeed indicate that the bands at 1277 and 1286 cm^{-1} arise from some mixing between $C_{\alpha 1}H_{2t}$ and peptide vibrations (CN_s, $C_{\alpha 1}C_s$), which also normally contribute to the eigenvector of amide III. The degree of mixing, however, depends on the molecule's protonation state and may thus obfuscate the identification of amide III. For the sake of simplicity, we designate the above bands of the zwitterionic state as amide III$_1$ (AIII$_1$) and amide III$_2$ (AIII$_2$) throughout the remaining part of the paper.

The above multiplicity should be absent in the spectra of AGL due to the absence of $C_{\alpha 1}H_{2t}$. This is in agreement with the

Dipeptides Probed by Raman Spectroscopy

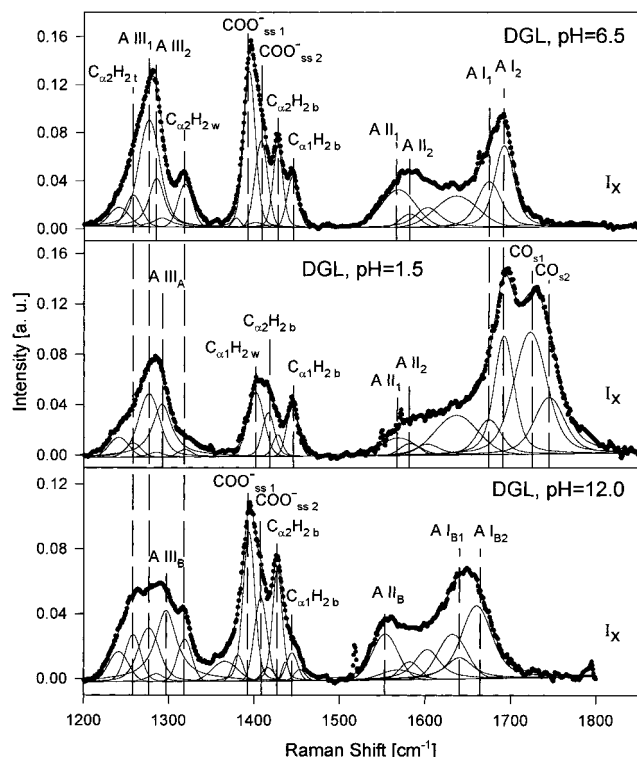*J. Phys. Chem. B, Vol. 103, No. 2, 1999* **379**

Figure 8. Parallel (*x*) polarized Raman spectra of DGL at pH 6.5, 1.5, and 12.0 recorded between 1200 and 1850 cm^{-1}. The dotted lines represent the experimentally observed spectra; the solid lines result from the fit to the data. The spectra were measured with 363.8 nm (cw) excitation.
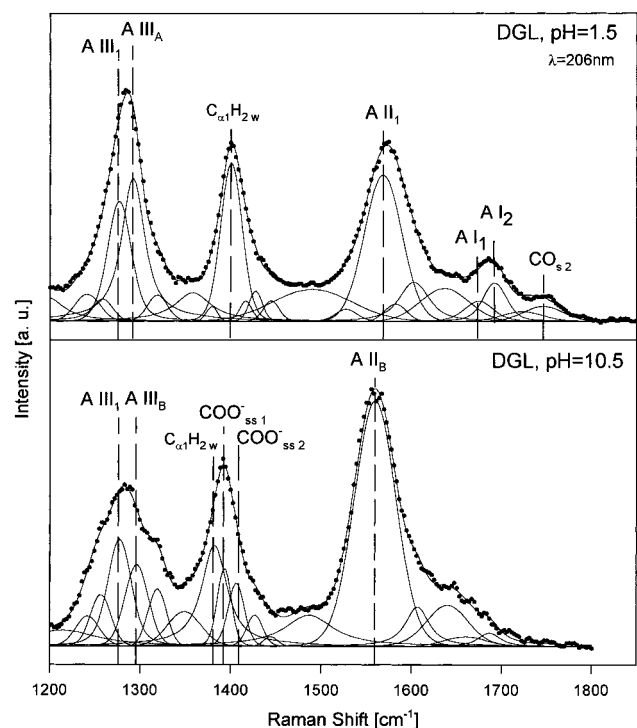

Figure 9. UV−resonance Raman of DGL in aqueous buffer adjusted to pH 1.5 and 10.5. The spectra were recorded with 206 nm excitation. A reference spectrum of the buffer was taken under the same conditions and subtracted from the originally measured Raman spectra. The most prominent Raman bands are indicated.

experiment, which reveals a single comparatively narrow amide III band at 1299 cm^{-1} in the spectra of deprotonated AGL (Figure 7).
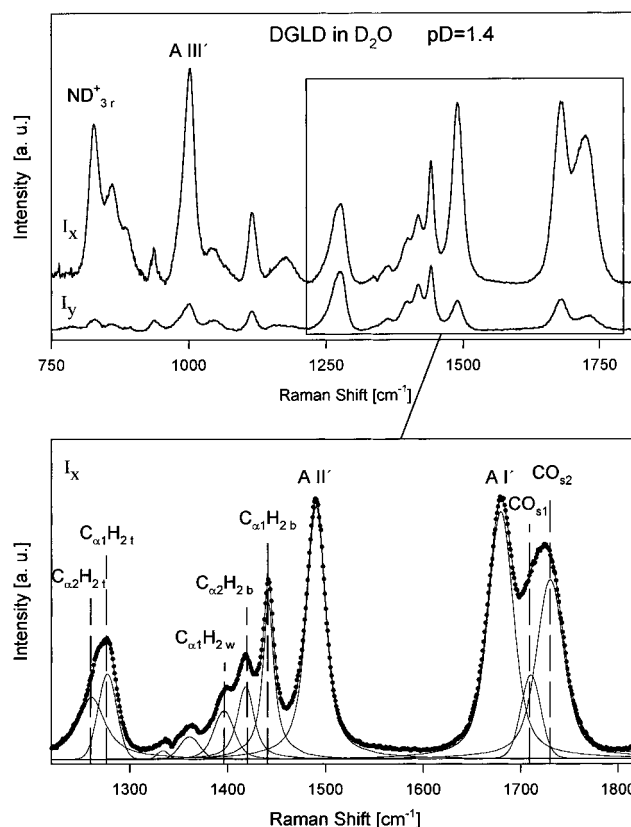

Figure 10. (Upper panel) polarized Raman spectrum of DGLD in D$_2$O (*x* and *y*, $\lambda = 500$ nm) measured with visible excitation wavelength at pD = 1.4. (Lower panel) spectral decomposition of the parallel (*x*) polarized DGLD spectrum at pD = 1.4 recorded between 1250 and 1800 cm^{-1}. The dotted lines represent the experimentally observed spectra; the solids lines result from the fit to the data.

The more isolated band at 1319 cm^{-1} in the DGL spectra (Figures 6 and 8), which is slighty downshifted by the NH ↔ ND exchange and observed at 1325 cm^{-1} in the AGL spectra (Figure 11), is assigned to C$_{\alpha2}$H$_{2w}$ (wagging). The band is depolarized in the DGL spectrum but becomes more polarized by NH ↔ ND exchange. Interestingly, it still appears as a shoulder of amide III with UV−resonance excitation and becomes less depolarized at 244 nm ($\rho = 0.45$, Chen et al., unpublished results). Chen et al.[7a] assigned this band to C$_{\alpha2}$H$_{2b}$.[21] However, as outlined above, the present study identifies the methylene bending modes at much higher frequencies. Instead, by utilizing again the normal coordinates of TGL, we attribute the 1319 and 1325 cm^{-1} bands of DGL and AGL to C$_{\alpha2}$H$_{2w}$.

It is noteworthy in this context, that earlier studies have already revealed a multiplet structure for the amide III band of (poly)peptides. Diem et al.[17a,19] have combined visible Raman, IR, and vibrational circular dichroism with normal coordinate calculations to analyze the amide III region of various diastereomeric forms of alanylalanine. In accordance with earlier studies by Krimm and Bandekar[20] that provided evidence that the amide III vibration primarily involves mixing between NH$_b$ and C$_\alpha$H$_b$ modes of the adjacent α-carbons. In contrast to the amide III of NMA little coupling between NH$_b$ and CN$_s$ occurs in polypeptides. Correspondingly, a vibrational analysis of TGL crystalls by Sundius et al.[17b] yielded mixing between NH$_b$ and C$_\alpha$H$_{2t}$ as predominantly determining the normal mode composition of amide III. Apparently, that does not apply to DGL. While our data indeed suggest that NH$_b$ couples to C$_\alpha$H$_{2tw}$, the resonance enhancement of AIII$_1$ in the zwitterionic state show, that coupling to CN$_s$ is still present. As we will show below,
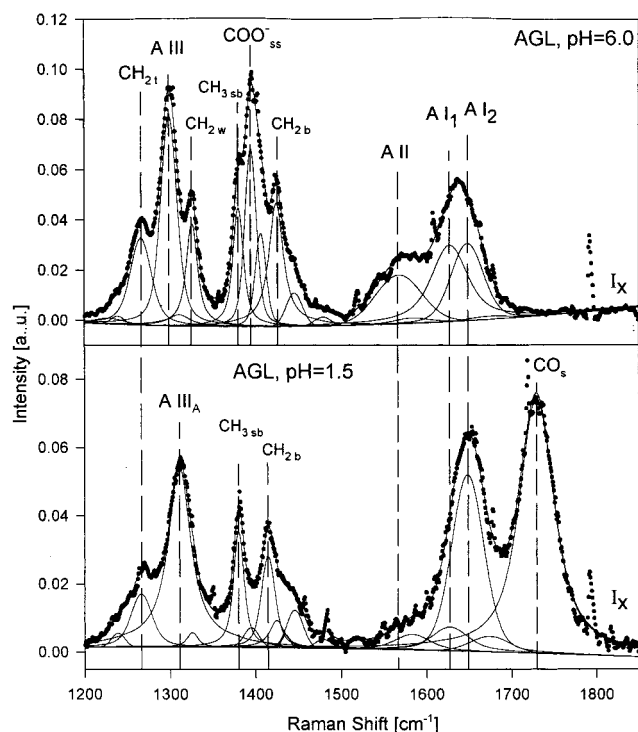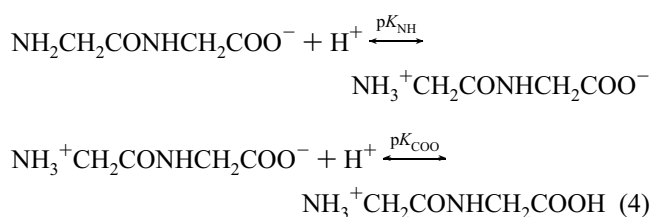
Figure 11. Parallel (*x*) polarized Raman spectra of AGL at pH 6.0 and 1.5 recorded between 1200 and 1850 cm^{-1}. The dotted lines represent the experimentally observed spectra; the solid lines result from the fit to the data. The spectra were obtained with 363.8 nm (cw) excitation.

the situation is even more complicated in the fully protonated and deprotonated states.

pH Dependence of Amide, Carboxylate, and Methylene Raman Bands. To explore the influence of the terminal charges on the vibrational dynamics, we have measured the polarized Raman spectra of DGL and AGL between pH 1.5 and 12.0. Figure 8 compares the non resonance Raman spectra of DGL measured at pH 6.5, 1.5, and 12.0. Figure 10 shows the polarized non resonance Raman spectra of DGLD at pD = 1.4. Figure 9 exhibits UV−resonance Raman spectra of DGL measured at pH 1.5 and 10.5 and Figure 11 depicts non resonance Raman spectra of AGL recorded at 6.0 and 1.5. From the analysis of various non resonance Raman spectra, we obtained the Raman titration curves for all relevant bands between 1200 and 1800 cm^{-1}, which are shown in Figures S5−S9. Raman bands of the same vibration with different frequencies in different protonation states (i.e., AIII$_2$, AII$_1$, AI$_1$, AI$_2$) were explicitly dealt with by the spectral analysis for all spectra investigated. They appear separately in Figures S5-S9 (cf. for instance the titration curves of AI$_{B1}$ and AI$_{B2}$, which reflect the deprotonated state, and of AI$_1$ and AI$_2$, which appear in the zwitterionic and in the fully protonated state).

These data were further analyzed by a simple titration model that involves the following reaction scheme for DGL:

$$NH_2CH_2CONHCH_2COO^- + H^+ \xrightleftharpoons{pK_{NH}}$$

$$NH_3^+CH_2CONHCH_2COO^-$$

$$NH_3^+CH_2CONHCH_2COO^- + H^+ \xrightleftharpoons{pK_{COO}}$$

$$NH_3^+CH_2CONHCH_2COOH \quad (4)$$

Since $pK_{NH} \gg pK_{COO}$, we neglect the titration state with a

protonated carboxylate and a deprotonated N-terminal group. The total intensity of a Raman band now reads as sum of the corresponding intrinsic intensities I_j of each titration state j, i.e., the deprotonated ($j = 1$), the zwitterionic ($j = 2$), and the fully protonated state ($j = 3$). The apparent band intensity reads as

$$I^{eff} = \sum_{j=1}^{3} \chi_j I_j \quad (5)$$

where the molar fraction χ_j of the above titration states can be expressed as function of pH and the pK values of the terminal groups by using the formalism in ref 22.

Equation 5 was successfully utilized to fit all experimentally obtained titration curves of DGL with the same pK values. This yielded pK_{NH} = 8.2 ± 0.2 and pK_{COO} = 3.5 ± 0.2. The fits are represented by the solid lines in Figure S5 up to S9. It should be emphasized that identical pK values were used to fit the titration curves of the subbands of COO$^-_{ss}$ and amide II, respectively. This indicates that the conformational transition between them does not change the pK values of the different groups.

In the following we list some of the major changes of frequencies and intensities as induced by the protonation/deprotonation of the terminal groups.

Protonation of the Carboxylate Group. The polarized spectra measured at pH 1.5 reflect a fully protonated DGL with a neutral carbonyl C-terminal. Instead of the COO$^-_{ss}$ and COO$^-_{as}$ bands, these spectra display a rather strong band at 1730 cm^{-1} band which results from the carbonyl CO$_s$ of the carboxyl end group (Figure 8). The spectral analysis clearly reveals that it is composed of two polarized subbands at 1723 (CO$_{s1}$) and 1745 cm^{-1} (CO$_{s2}$), which we assign to two different orientations of the carbonyl group with respect to the peptide plane. The same result was obtained for DGLD at pD 1.4 (Figure 10). The intensities of both subbands are relatively weak with UV excitation, but the analysis of the corresponding UV−resonance Raman spectrum in Figure 9 reveals that CO$_{s2}$ exhibits more intensity in contrast to the situation with visible and near UV excitation (Figure 8). In contrast, CO$_s$ of AGL can be fit with a single broad band at 1729 cm^{-1} (Figure 11).

Interestingly, the carboxylate protonation has no clearly discernible effect on the amide I subband frequencies of both DGL and AGL (we do not rule out a slight upshift), while it significantly increases the intensity of the respective AI$_2$ subbands (Figures 8 and 11). The intensity of AI$_1$ is slightly enhanced for DGL but dramatically reduced for AGL, so that amide I nearly appears as a single band (cf. Figures 8, 11, and S5). For both peptides the amide II intensities decrease so that their (sub)bands are barely detectable with nonresonance excitation (Figures 8, 11, and S6). This parallels findings by Chen et al.,[7a] who found that the protonation of AGL reduces the UV−resonance Raman intensity of amide II by a factor of 3.

As already mentioned in the preceeding section, amide III shows a more complex behavior. For DGL the carboxylate protonation reduces AIII$_1$ by a factor of about 2, while AIII$_2$ disappears and is replaced by a "new" and even stronger amide III$_A$ band at 1291 cm^{-1} (Figure 8 and S3). For AGL, protonation replaces the 1299 cm^{-1} band by a band at 1311 cm^{-1}, which is again more intense.

While only AIII$_1$ appears resonance enhanced in the zwitterionic state, both the amide III$_1$ and the amide III$_A$ subbands gain intensity in the fully protonated state of DGL (Figure 9). In fact, AIII$_A$ is now more enhanced than AIII$_1$. This may result from admixtures of NC$_{\alpha s}$, CN$_s$, and CO$_s$ to the AIII$_2$ vibration,

Dipeptides Probed by Raman Spectroscopy

J. Phys. Chem. B, Vol. 103, No. 2, 1999 **381**

which would facilitate vibronic coupling to the two lowest $\pi \rightarrow \pi^*$ transitions of the peptide group.

As already mentioned, all carboxylate bands of DGL and AGL disappear at acid pH, in line with expectations (Figures 8−11 and S9). In parallel, their $C_{\alpha2}H_{2\ b}$ bands shift to lower frequencies, i.e., from 1427 to 1416 cm^{-1} for DGL and from 1425 to 1415 cm^{-1} for AGL, and their depolarization ratios increase significantly (from 0.33 to 0.6 for DGL and AGL). This strongly indicates vibrational mixing with COO$^-_{ss}$.

As mentioned above, we identified in DGL another polarized band at 1399 cm^{-1}, which we assigned to $C_{\alpha1}H_{2w}$. The deuteration of the NH group decreases its intensity, depolarizes the band, and shifts it to slightly lower frequencies (1395 cm^{-1}) (Figure 10). All this indicates vibrational mixing with some peptides and/or backbone vibrations. The 1424 cm^{-1} band loses two-thirds of its intensity, while the Raman band of the other methylene band of DGL at 1444 cm^{-1} slightly increases with acid pH (Figure S8).

Deprotonation of the Ammonium Ion of DGL. As shown in Figures 8 and 9, the deprotonation of the N-terminal group drastically downshifts both amide I subbands. Their frequency positions are now obtained at 1640 and 1660 cm^{-1}, and the intensities are slightly reduced (Figure S5). For amide II AII$_2$ remains nearly unaffected, while the respective low-frequency component AII$_1$ disappears and is replaced by a relatively pronounced band at 1554 cm^{-1} (Figure S6). The intensity of AIII$_1$ is reduced by more than a factor of 3, but its frequency is unchanged (Figures 8 and 9). In contrast, AIII$_2$ disappears and is replaced by an even stronger polarized band at 1296 cm^{-1}. The COO$^-_{ss}$ bands lose about 25% of their intensities (Figure S9). Interestingly, this is not accompanied by any significant changes of their depolarization ratio. In line with expectations neither the intensities nor the frequencies of the C-terminal methylene ($C_{\alpha2}H_2$) modes are significantly affected by the ammonium deprotonation, whereas the intensity and the depolarization ratios of the $C_{\alpha1}H_2$ band were found to decrease (Figure S8).

The UV−resonance Raman spectrum measured at pH = 10.5 also shows a broad amide III band with significant contributions of AIII$_1$ and AIII$_2$ (Figure 9). Additionally, the $C_{\alpha2}H_{2\ t}$ band at 1258 cm^{-1} also gains some resonance intensity, so that it contributes to the total amide III band shape. Taken together the above results show that both penultimate charges significantly impact on the structure and the vibrational dynamics of the peptide ground state.

Discussion

The analysis of the Raman titration curves revealed that the positive charge of the ammonium group causes the carboxyl group to shift its pK value from 4.0 (in AGL) to 3.5 (in DGL), presumably due to Coulombic interactions between the two charges (Figures S5-S9). Assuming unrestricted solvent accessibility for the terminal charges Z_{NH} and Z_{COO}, the Tandford−Kirkwood theory[23a,b] predicts the following relationship between the electrostatic potential and the induced pK shift:

$$U_{NC} = 2.303kTZ_{NH}Z_{COO}(pK_{int} - pK) \tag{6}$$

pK_{int} is the pK value of the unperturbed group, i.e., in our case the carboxylate in AGL. In a rough estimation U_{NC} may be considered as resulting from the Coulomb interaction between two opposite charges separated by bulk water ($\epsilon = 80$). In this case the distance between the charges may be estimated by inserting eq 6 into

$$R_{NC} = \frac{Z_{NH}Z_{COO}e^2}{4\pi\epsilon_0\epsilon U_{NC}} \tag{7}$$

Inserting the experimentally obtained pK values, we obtain $R_{NC} = 6.0$ Å. Only slightly larger values are obtained by taking into account higher order reaction field contributions generated by the interaction of the above charges with the dielectric continuum of the solvent.[23c] Hence our data indicate that the end groups are oriented in a way that ensures a minimal distance between them. Since the pK values of both end groups were found to be identical for the COO$^-_{ss}$ and amide II subbands, we conclude that they reflect conformations with nearly the same end to end distances.

The above estimation agrees well with conclusions drawn from NMR experiments on GlyAla and AlaGly dipeptides reported by Beeson and Dix.[6] The molecular mechanics calculations performed by these authors yielded several possible conformers that differ with respect to the peptide's dihedral angles. Two of them would be consistent with the above requirements, i.e., close and nearly identical distances (5 Å in their calculations) between the charges. Rotamer R$_1$ has both end groups cis to the peptide's carbonyl, while their respective orientation is trans in R$_2$. Hence, one would presume that the two conformers inferred from the COO$^-_{ss}$, CO$_s$, and amide II subbands are assignable to the above rotamers. Two experimental findings, however, rule out this possibility. We have measured UV−resonance Raman spectra of DGL at different temperatures between 25 and 84 °C. While a spectral shift is revealed for both the COO$^-_{ss}$ and amide II band, no band shape changes are detectable (data not shown). This shows that the occupation numbers of the conformers do not change over the above temperature interval. Hence the free energy difference between them must be very small. In view of the study by Beeson and Dix[6] this is unlikely to be the case for conformations with different dihedral angles. Second, we found that the intensity ratio of the COO$^-_{ss}$ subbands is nearly identical for DGL and AGL. This is unexpected for the rotamers because their free energy difference should significantly depend on whether the other terminal group is charged or not.

In this context it is useful to further characterize the subbands of COO$^-_{ss}$. To this end we invoke the peptide−carboxylate electronic interaction recently observed by Asher and co-workers.[7] As mentioned earlier, their studies have provided conclusive evidence that electronic coupling between the carboxylate's and peptide's antibonding π^* orbitals yield two mixed excited states π_a^* and π_b^*. However, the former is still dominated by the amide orbital, whereas the latter is predominatly carboxylate. The ground states of both groups were assumed to be totally localized. A schematic energy level diagram is depicted in Figure S10.

The partially delocalized character of the lowest excited states allows charge-transfer transitions from the carboxylate to the peptide and vice versa. Chen et al.[7a] have invoked a charge-transfer transition from the nonbonding orbital n$_{COO}$ to state π_A^* (CT$_n$) to explain the pH dependence of optical absorption around 190 nm and the strong resonance enhancement of COO$^-_{ss}$ with 218 and 244 nm excitation. In the preresonance and nonresonance region, scattering by this transition interferes with contributions from the nearly intrinsic $\pi_{COO} \rightharpoonup \pi_b^*$ transition of the carboxylate. By proposing this interference, one can nicely explain the depolarization ratio value of 0.5 for the COO$^-_{ss}$. This charge-transfer transition CT$_n$ changes the carboxylate to a neutral radical, which causes its C−O bonds to contract. In parallel, the amide CO and CN bonds expand

due to the occupation of an antibonding orbital. The $\pi_{COO} \rightarrow$ p_b^* transition is unlikely to affect the amide bonds and will solely expand the carboxylate bonds, since π_b^* is of antibonding character. Hence, the Franck–Condon integrals have opposite signs for both transitions, yielding a depolarization ratio intermediate between 0.33 and 0.75 (eqs 2 and 3), depending on the relative strength and the direction of the dipole transitions as well as on the respective vibronic coupling efficiency.

The COO^-_{ss1} band at 1396 cm^{-1} fits nicely into this picture in that it shows $\rho \approx 0.5$ even with nonresonance excitation. This is not the case for the other subband, which appears polarized with $\rho = 0.29$ in the near UV region. Polarized UV–Raman spectra taken with 244 nm excitation indicate that its depolarization ratio is close to 0.33 (Chen et al., unpublished data). This suggests that CT_n contributes much less to this band compared with COO^-_{ss1}. To explain the experimentally observed depolarization ratio for the COO^-_{ss2} subband, we invoke different rotational states of the carboxylate plane with respect to the peptide plane. If both planes are parallel, the overlap between the n_{COO} and $\pi_{peptide}$ orbitals is small because of their perpendicular orientation. One, therefore, expects that the probability of CT_n is weak in this conformation. However, because of the parallel orientation of the respective p_z orbitals one may presume a CT between the π_{COO} and π_a^* orbitals to be operative, which we designate as CT_π in the following. It would cause an expansion of the carboxylate bonds because it creates a hole in the bonding π_{COO} orbital. Hence, the Franck–Condon factor would have the same sign as for $\pi_{COO} \rightarrow \pi_b^*$, so that its interference with CT_π would cause a polarized band with $\rho < 0.33$ in the nonresonance region, in accordance with our experimental findings for the COO^-_{ss2} subband.

In contrast, the depolarization ratio of COO^-_{ss1} suggests that CT_n contributes to its Raman cross section. This electronic interaction is most effective when the carboxylate group exhibits a nearly perpendicular orientation with respect to the peptide plane. In this case, the nonbonding n_{COO} orbital is oriented parallel to the p_z orbitals of the peptide. This allows an overlap between the n_{COO} and π_a^*.

On the basis of above considerations, we conclude that the two COO^-_{ss} subbands reflect different torsional angles, τ, between the carboxylate and the peptide plane. While the higher frequency band results from a conformation in which the carboxylate is parallel oriented to the peptide group, the lower frequency band is assignable to a more distorted geometry in which τ differs significantly from zero. It should be mentioned that the single crystal investigated by Pajcini et al.[7b] exhibits a structure with a significant torsional angle between carboxylate and peptide. Consequently, one obtains a COO^-_{ss} band that becomes resonance enhanced by the CT_n transition.

While the above model explains the different depolarization ratios of the COO^-_{ss} subbands, it does not directly account for the frequency differences. One possible explanation invokes two distinguishable subconformations[24] with $\tau = 0$ and $\tau = 90°$, which may coexist for the trans- as well as for the cis-rotamer of the carboxylate. For the trans-rotamer of the peptide it is possible that the former is stabilized by hydrogen bonding between the carboxylate and the NH bond. In the perpendicular subconformer, however, the carboxylate is certainly hydrogen bonded to water molecules.[7b] Both types of hydrogen bonds are of comparable strength, so that the two subconformers can be assumed to be nearly isoenergetic, in accordance with the absence of any temperature dependence. The frequency difference may result from the fact that vibrational mixing between COO^-_{ss} and peptide vibrations is more facilitated for the

subconformer with $\tau = 0$. It is also reasonable to assume, that COO^-_{ss} is anharmonically coupled to the torsional motion of the carboxylate, which would give rise to a τ dependence of the COO^-_{ss} frequency.

As an alternative to invoking two distinguishable subconformations, one may assume a broad distribution of the carboxylate orientations. Anharmonic coupling would then lead to a continuous mapping of τ onto the band shape, so that the latter would be composed of numerous indistinguishable subbands. This requires significant rotational flexibility of the carboxylate. Indeed, a computational study on a protonated glycine–$(H_2O)_4$ complex suggests a coexistence between a trans and cis conformation of the carboxylate group.[25] Moreover, a recent paper by Godfrey and Brown[26] reports a large degree of flexibility along the torsional coordinate τ of isolated protonated glycine. Hence, one may invoke a very shallow potential minimum with respect to τ centered around 90° (perpendicular orientation), which only increases for angles approaching either 0 or 180°. This is very similar to a box potential. Thus the eigenfunctions can be approximated by $\sqrt{2/\pi} \sin n\, \tau$, so that the mean square displacement $\langle\tau\rangle^2$ is independent of the quantum number n and consequently also of the temperature. If one assumes that the COO^-_{ss} is anharmonically coupled to τ, the latter is mapped onto the frequency of the former to yield a temperature independent broadening. Moreover, one expects that in the case of such a shallow potential the torsional motion is very slow so that conformational averaging within the lifetime of the COO^-_{ss} vibrational state is at least partially avoided. This would be a prerequisite for the observation of an asymmetric band shape.[27]

We now discuss the influence of the carboxylate protonation on other bands in the Raman and IR spectra of AGL and DGL. First we deal with amide III of DGL. The depolarization ratios of both amide III subbands increase upon carboxylate protonation. At neutral pH AIII$_1$ has $\rho = 0.26$ with near and far UV excitation suggesting two tensor components with the same sign, which result from vibronic coupling to NV$_1$ as well as to CT_n and/or CT_π. Protonation eliminates the latter, thus causing the depolarization ratio to increase to 0.33. The high-frequency subband exhibits $\rho = 0.13$ with 363 nm excitation at neutral pH, which is indicative of two nearly identical or three different tensor components with the same sign. Carboxylate protonation substitutes this band by another one (AIII$_A$) at higher frequencies with a different band shape and a larger depolarization ratio (0.2). All these changes suggest a somewhat different normal composition compared with AIII$_2$.

Unfortunately, the situation is less clear for AGL. While COO^-_{ss} clearly appears as a doublet, amide II and III can be fitted by single Gaussian bands. Amide III is significantly upshifted from 1299 to 1311 cm^{-1} upon carboxylate protonation. The depolarization ratio slightly increases from 0.21 to 0.33. As for DGL this results from the elimination of the CT transition. Interestingly, there is a discrepancy between the pH dependence of amide III in this and the UV–Raman study of Chen et al.[7a] While the latter reports a nearly 3-fold decrease with carboxylate protonation we found only a slighty reduction of the intensity with visible excitation. This indicates that different coupling mechanisms determine the visible and the UV–Raman tensor.

Dipeptides Probed by Raman Spectroscopy

J. Phys. Chem. B, Vol. 103, No. 2, 1999 **383**

In contrast to the amide III subbands, the multiplicity of amide II is unlikely to arise from vibrational mixing with nonpeptide vibrations, since it appears as a single band in the single-crystal spectra. Since the amide II subbands do not show any temperature dependence of its intensity ratio between 20 and 85° C, we assign them to the COO^- rotamers introduced above.

Amide II loses most of its intensity with acid pH. This effect is even stronger than observed with UV excitation, where Chen et al. observed a 3-fold decrease. Both results suggest that at least one of the above charge-transfer transitions provides a predominant constructive contribution to the Raman tensor.

Interestingly, the ammonium deprotonation also upshifts $AIII_2$ ($AIII_2 \rightarrow AIII_B$). Moreover, its intensity is slightly enhanced. In contrast, $AIII_1$ remains unshifted but loses around 60% of its intensity. While AII_2 remains nearly unaffected, AII_1 shifts down without drastic changes of its intensity. Both COO^-_{ss} bands show a slight but clearly discernible decrease of their intensities. Altogether, these observations suggest that the ammonium deprotonation reduces the CT_n and CT_π contribution to the Raman tensor of the above bands and causes their intensities to decrease. This is in particular obvious for $AIII_1$ and $AIII_2$, for which the depolarization ratio increases in a similar way as observed for acid pH.

It is of relevance to note in this context that amide I in DGL is most strongly affected by the ammonium deprotonation. Both subbands are drastically downshifted (1674 to 1640 cm^{-1} and 1692 to 1660 cm^{-1}). Additionally, the AI_1 intensity decreases by a factor of 2. The physical basis for the above observations is not absolutely clear, but one may interpret them as indicative of an increase in the hydrogen bonding strength to the adjacent water molecules for the following reasons. First, it is well established that the amide I frequency is a measure of hydrogen bonding interaction in that its frequency decreases upon an increased hydrogen bonding, whereas the intensity decreases with preresonance excitation. Second, it is known that the protonated ammonium stabilizes a specific rigid structure of its aqueous environment,[6] which is certainly rearranged upon deprotonation. Hydrogen bonding between water and carbonyl groups may well be altered as a consequence of these changes.

An alternative explanation may be given by invoking a vibrational Stark effect, i.e., an upshift of the oscillator frequency in the electric field of the ammonium group. Vibrational Stark effects have frequently been reported for CO groups in various environments.[28]

The high-frequency value of amide I may in part result from some vibrational coupling with $NH_{3\ ab}$. This would explain the somewhat lower frequency in the spectrum of DGLD, in which the corresponding $ND_{3\ ab}$ is at much lower frequencies. Invoking this interaction, however, does not explain that the average amide I frequency is 1645 cm^{-1} for the observed doublet in the spectra of DGL crystals (Figure S4). The huge splitting of the latter is another mystery, since it can hardly arise from interpeptide transition dipole coupling.[29] Hence, there are some open questions concerning the understanding of amide I of DGL and similar dipeptides, which are the subject of future investigations.

Summary

This study presents for the first time a detailed analysis of the vibrational spectra of the model peptides DGL and AGL in H_2O and D_2O for different protonation states of their terminal groups. A self-consistent global fit to polarized normal Raman, UV−resonance Raman, and FTIR spectra measured at various pH values aimed at identifying and characterizing even strongly overlapping bands between 800 and 1700 cm^{-1}. The thus obtained frequencies and relative intensities of Raman and IR bands provide a basis for a normal coordinate analysis. The most imporatant results emerging from our work are as follows.

(1) The carboxyl stretch band at 1400 cm^{-1} is composed of two subbands (1394 and 1408 cm^{-1} for DGL, 1395 and 1406 cm^{-1} for AGL) with significantly different depolarization ratios. They remain nearly unaffected by the deuteration of the peptide group in D_2O. In contrast, only a single band appears in the spectra of DGL crystals. The subbands were assigned to different subconformers with respect to the torsional coordinate of the carboxylate group. The different depolarization ratios are interpreted as reflecting vibronic coupling to different charge-transfer transitions from the carboxylate orbitals n_{COO} and π_{COO} into the first excited π^* state of the peptide group. While the former is likely to occur if the carboxylate is parallel to the peptide, the latter probably derives from a perpendicular orientation.

(2) The above conformers give rise to an amide II doublet in the DGL spectra (1561 and 1584 cm^{-1}), which merges to a broad single band at 1568 cm^{-1} in the spectra of AGL.

(3) For DGL, amide III shows two subbands at 1277 and 1285 cm^{-1} in the normal and FTIR spectra. In the UV−resonance Raman spectra, only the low-frequency subband is significantly enhanced. In the fully protonated and deprotonated state, however, both subbands are resonance enhanced. Additionally, a band at 1258 cm^{-1} gains significant intensity in the normal as well as in the UV−Raman spectra. This complex composition of amide III cannot result from conformational heterogeneity, since it is still present in the spectra of DGL crystals. We attribute it to vibrational mixing between twisting vibrations of the two methylenes and stretching vibrations of the peptide, which are known to be coupled to its $\pi \rightarrow \pi^*$ transition.

(4) As reported in a previous study,[10] amide I of DGL and AGL is a doublet that arises from vibrational mixing with water. For DGL, the amide I band exhibits a rather high frequency (1690 cm^{-1}) very close to values obtained for peptides in a vacuum. It downshifts to more common values upon deprotonaton of the ammonium group. This points to a strong influence of the N-terminal group on the CO bond strength, which is presently not understood.

Note Added in Proof. Only after this paper was already accepted did we become aware of a recent study by Serrano-Andrés and Fülscher.[30] These authors employed the Complete Active Space (CAS) SCF method and multiconfigurational second-order perturbation theory (CASPT2) to calculate various transitions into excited electronic states of an *N*-acetyl-*N'*-methylglycylamide dimer. Thus, they obtained theoretical evidence for charge transfer transitions between the n and π orbitals of one peptide into the π^* state of the other one. Their oscillator strengths were found to strongly depend on the orientation of the peptide groups with respect to each other in that $\pi \rightarrow \pi^*$ is predominant for parallel oriented peptides, while $n \rightarrow \pi^*$ is preferred for a configuration with perpendicular orientation. Apparently, these findings are in close correspondence to our model for the orientational dependence of the n

384 *J. Phys. Chem. B, Vol. 103, No. 2, 1999*

Sieler et al.

→ π* and π → π* charge transfer transitions between the carboxylate and peptide group of AGL and DGL.

Supporting Information Available: Tables S1−S4 contain all spectral parameters obtained by the self-consistent analysis for DGL, DGLD, AGL, and AGLD. Figures S1 and S2 show the polarized Raman and FTIR spectra of DGL, DGLD, AGL, and AGLD measured with visible excitation wavelengths at neutral pH/pD. Figure S3 contains the UV−resonance Raman spectrum of DGL with 206 nm excitation and Figure S4 the polarized UV−preresonance ($\lambda = 244$ nm) and visible Raman spectra ($\lambda = 488$ nm) of single-crystal DGL. Figures S5-S9 depict the Raman titration curves of the amide I, II, III, COO_{ss}, and CH_2 modes of DGL and AGL analyzed by a simple titration model outlined in the text. Figure S10 illustrates the schematic energy level diagram of the amide and carboxyl orbitals. This information is available free of charge via the Internet at http://pubs.acs.org.

References and Notes

(1) (a) Miyazawa, T.; Shmanouchi, T.; Mizushima, S.-I. *J. Chem. Phys.* **1956**, *24*, 408. (b) Dudik, J. M.; Johnson, C. R.; Asher, S. A. *J. Phys. Chem.* **1985**, *89*, 3805. (c) Krimm, S.; Bandekar, J. *Adv. Protein Chem.* **1986**, *38*, 181. (d) Jordan, T.; Spiro, T. G. *J. Raman Spectrosc.* **1995**, *26*, 867. (e) Markham, L. M.; Hudson, B. S. *J. Phys. Chem.* **1996**, *100*, 2731.

(2) (a) Chen, X. G.; Schweitzer-Stenner, R.; Mirkin, N. G.; Krimm, S.; Asher, S. A. *J. Am. Chem. Soc.* **1994**, *116*, 11141. (b) Chen, X. G.; Schweitzer-Stenner, R.; Asher, S. A.; Mirkin, N. G.; Krimm, S. *J. Phys. Chem.* **1995**, *99*, 3074. (c) Asher, S. A.; Li, P.; Chi, Z.; Schweitzer-Stenner, R.; Mirkin, N. G.; Krimm, S. *J. Phys. Chem*, **1997**, *101*, 3992.

(3) (a) Mirkin, N. G.; Krimm, S. *J. Mol. Struct.* **1991**, *242*, 143. (b) Mirkin, N. G.; Krimm, S. *J. Am. Chem. Soc.* **1991**, *113*, 9742. (c) Mirkin, N. G.; Krimm, S. *J. Mol. Struct.* **1996**, *377*, 219.

(4) (a) Bradley, E. K.; Thomason, J. F.; Cohen, F. E.; Kosen, P. A.; Kuntz, I. D. *J. Mol. Biol.* **1990**, *215*, 697. (b) Dyson, H. J.; Rance, M.; Houghten, R. A.; Lerner, R. A.; Wright, P. E. *J. Mol. Biol.* **1988**, *202*, 161. (c) Schafer, L.; Newton, S. Q.; Cao, M.; Peeters, A.; van Alsenoy, C.; Wolinski, K.; Momany, F. A. *J. Am. Chem. Soc.* **1993**, *115*, 272. (d) Blatt, H. D.; Smith, P. E.; Pettitt, B. M. *J. Phys. Chem. B* **1997**, *101*, 7628.

(5) (a) Rao, S. N.; Parthasarathy, R. *Acta Crystallogr.* **1973**, *B29*, 2379. (b) Koetzle, T. F.; Hamilton, W. C.; Parthasarathy, R. *Acta Crystallogr.* **1972**, *B28*, 2083. (c) Biswas, A. B.; Hughes, E. W.; Sharma, B. D.; Wilson, J. N. *Acta Crystallogr.* **1968**, *B24*, 40.

(6) Beeson, C.; Dix, T. A. *J. Chem. Soc., Perkin. Trans. 2* **1991**, 1913.

(7) (a) Chen, X. G.; Li, P.; Holtz, J. S. W.; Chi, Z.; Pajcini, V.; Asher, S. A.; Kelly, L. A. *J. Am. Chem. Soc.* **1996**, *118*, 9705. (b) Pajcini, V.; Chen, X. G.; Bormett, R. W.; Geib, S. J.; Asher, S. A. *J. Am. Chem. Soc.* **1996**, *118*, 9716.

(8) (a) Chakrabborty, D.; Yash, A.; Manogaran, S. *J. Mol. Struct.* **1994**, *303*, 265. (b) Chakrabborty, D.; Manogaran, S. *J. Phys. Chem A* **1997**, *101*, 6964.

(9) Lagant, P.; Vergoten, G.; Loucheux-Lefebvre, M. H.; Fleury, G. *Biopolymers* **1983**, *22*, 1269.

(10) Sieler, G.; Schweitzer-Stenner, R. *J. Am. Chem. Soc.* **1997**, *119*, 1720.

(11) (a) Long, D. A. *Raman Spectroscopy*; McGraw-Hill: Great Britain, 1977. (b) Myers, A. B.; Mathies, R. A. *Biological Applications of Raman Spectroscopy*; Spiro, T. G., Ed.; John Wiley & Sons Inc.: New York, 1987; Vol 2, p 1. (c) Albrecht, A. C.; Hutley, M. C. *J. Chem. Phys.* **1971**, 55, Number 9, 4438.

(12) Li, P.; Sage, J. T.; Champion, P. M. *J. Chem. Phys.* **1992**, *97*, 3214.

(13) Glasoe, P. K.; Long, F. A. *J. Phys. Chem.* **1960**, *64*, 188.

(14) Unger, E.; Dreybrodt, W.; Schweitzer-Stenner, R. *J. Phys. Chem. A* **1997**, *101*, 5997.

(15) Bevington, P. R. *Data Reduction and Error Analysis for the Physical Science*; McGraw-Hill: New York, 1969.

(16) This is justified by the fact that the parameters used to fit the Raman spectra of the DGL crystal taken with 488 nm could also be used to fit the corresponding spectra measured at 244 nm by convoluting their Lorentzian band shapes with a Gaussian of 10 cm^{-1} width.

(17) (a) Diem, M.; Polavarapu, P. L.; Oboodi, M.; Nafie, L. A. *J. Am. Chem. Soc.* **1982**, *104*, 3329. (b) Sundius, T.; Bandekar, J.; Krimm, S. *J. Mol. Struct.* **1989**, *214*, 119. (c) Qian, W.; Bandekar, J.; Krimm, S. *Biopolymers* **1991**, *31*, 193. (d) Williams, R. D.; Kalasinsky, V. F.; Lowrey, A. H. *J. Mol. Struct.* **1993**, *281*, 157. (e) Qian, W.; Krimm, S. *J. Phys. Chem.* **1994**, *98*, 9992. (f) Yu, G.-S.; Freedman, T. B.; Nafie, L. A.; Deng, Z.; Polvarapu, P. L. *J. Phys. Chem.* **1995**, *99*, 835.

(18) Schweitzer-Stenner, R.; Sieler, G.; Mirkin, N. G.; Krimm, S. *J. Phys. Chem. A* **1998**, *102*, 118.

(19) (a) Oboodi, M. R.; Alva, C.; Diem, M. *J. Phys. Chem.* **1984**, *88*, 501. (b) Roberts, G. M.; Lee, O, Calienni, J.; Diem, M. *J. Am. Chem. Soc.* **1988**, *110*, 1749.

(20) Krimm, S.; Bandekar, G. M. *Biopolymers* **1980**, *19*, 1.

(21) The authors used the notation C_β instead of $C_{\alpha2}$. Normally, C_β labels the first carbon atom of an amino acid residue. The CH_2 exhibits only a single bending mode, so that there is no need to use the term symmetric for its characterization.

(22) Schweitzer-Stenner, R.; Wedekind, D.; Dreybrodt, W. *Biophys. J.* **1986**, *49*, 1077.

(23) (a) Tandford, C.; Kirkwood, J. G. *J. Am. Chem. Soc.* **1957**, *79*, 5333. (b) Matthew, J. B.; Hanania, G. I. H.; Gurd, F. D. N. *Biochem. Biophys. Res. Commun.* **1978**, *81*, 410. (c) Smith, P. E.; Pettit, B. M. *J. Phys. Chem.* **1994**, *98*, 8, 9700.

(24) We use the term "subconformation" when peptides have different conformations with respect to a structural coordinate other than the dihedral angles.

(25) Williams, R. G.; Kalasinsky, V. F.; Lowrey, A. H. *J. Mol. Struct.* **1983**, *281*, 157.

(26) Godfrey, P. D.; Brown, R. D. *J. Am. Chem. Soc.* **1995**, *117*, 2019.

(27) MacPhail, R. A.; Snyder, R. G.; Strauss, H. L. *J. Am. Chem. Soc.* **1980**, *102*, 3978.

(28) (a) Lampert, D. K. *J. Chem. Phys.* **1991**, *94*, 6237. (b) Marti, J.; Liedós, A.; Duran, M. *J Comput. Chem.* **1992**, *13*, 821. (c) Bishop, D. M. *J. Chem. Phys.* **1992**, *98*, 3179.

(29) Transition dipole coupling would cause splitting between the A_g and B_g type amide I modes of the crystal's unit cell, which has C_{2h} symmetry. Though Raman active in principle, a B_g mode is not able to gain intensity from Franck−Condon coupling to electronic states. Its Raman intensity should therefore much be less than that of the A_g mode, in contrast to the experimental data. Moreover, the Raman tensor of both amide I bands does not suggest that they arise form different symmetries. Finally, given the distance between adjacent petides, transition dipole coupling should not be able to cause a splitting of 40 cm^{-1}. In crystallized NMA, the corresponding splitting between the A_g and B_{2g} modes is 23 cm^{-1}. As expected, the band of the latter is weak and gets its intensity solely from some disorder of the crystal structure.[18]

(30) Serrano-Andrés, L.; Fülscher, M. P. *J. Am. Chem. Soc.* **1998**, *120*, 10912.